Liquid Crystals
Publication details, including instructions for authors and subscription information:
http://www.informaworld.com/smpp/title~content=t713926090

Anomalous behaviour in the SmA*-SmC$_A$* pre-transitional regime of a chiral swallow-tailed antiferroelectric liquid crystal

Surjya Sarathi Bhattacharyya[a]; M. Rahman[a]; A. Mukherjee[a]; B. K. Chaudhuri[a]; S. L. Wu[b]
[a] Department of Solid State Physics, Indian Association for the Cultivation of Science, Kolkata - 700032, India [b] Department of Chemical Engineering, Tatung Institute of Technology, Taipei 104

To cite this Article Bhattacharyya, Surjya Sarathi , Rahman, M. , Mukherjee, A. , Chaudhuri, B. K. and Wu, S. L.(2008) 'Anomalous behaviour in the SmA*-SmC$_A$* pre-transitional regime of a chiral swallow-tailed antiferroelectric liquid crystal', Liquid Crystals, 35: 6, 751 — 756
To link to this Article: DOI: 10.1080/02678290802130231
URL: http://dx.doi.org/10.1080/02678290802130231

Liquid Crystals,
Vol. 35, No. 6, June 2008, 751–756

Taylor & Francis
Taylor & Francis Group

Anomalous behaviour in the SmA*–SmC_A* pre-transitional regime of a chiral swallow-tailed antiferroelectric liquid crystal

Surjya Sarathi Bhattacharyya[a], M. Rahman[a], A. Mukherjee[a], B. K. Chaudhuri[a]* and S. L. Wu[b]

[a]*Department of Solid State Physics, Indian Association for the Cultivation of Science, Kolkata - 700032, India;* [b]*Department of Chemical Engineering, Tatung Institute of Technology, Taipei 104, Taiwan, R.O.C*

(Received 8 June 2007; final form 15 April 2008)

The temperature- and electric field-dependent dielectric relaxation and polarisation of a new chiral swallow tailed antiferroelectric liquid crystal, i.e. 1-ethylpropyl (*S*)-2-{6-[4-(4′-decyloxyphenyl)benzoyloxy]-2-naphthyl}propionate (abbreviated as EP10PBNP), were investigated. The electric field-induced dielectric loss spectra of EP10PBNP revealed electroclinic and anomalous dielectric behaviour in the chiral smectic A (SmA*)–chiral antiferroelectric smectic C (SmC_A*) pre-transitional regime. From an analysis of thermal hysteresis of the dielectric constant, electric field-induced polarisation and dielectric loss spectra, the appearance of a ferrielectric-like mesophase is observed followed by an unstable SmC_A* phase in the SmA*–SmC_A* pre-transitional regime.

Keywords: chiral swallow-tailed antiferroelectric liquid crystal; pre-transitional regime; dielectric anomaly; electroclinic effect

1. Introduction

Antiferroelectric liquid crystals (AFLCs) and their mixtures have been shown to exhibit thresholdless V-shaped switching properties (*1*) and thus have profound application potential in the display industry as well as in other electro-optical devices. In general, highly chiral molecular attachments to the mesogenic core of the molecule (*2*) and achiral swallow-tailed terminal moieties (*3, 4*) are the main reasons for the existence of an AFLC phase in a liquid crystal material. The first AFLC to be discovered, i.e. MHPOBC, exhibited three different phases while undergoing a paraelectric to antiferroelectric phase transition (*5–7*). However, another well-known antiferroelectric material, abbreviated as TFMHPOBC, exhibited a direct paraelectric to antiferroelectric transition (*8*). The phenomenological theory of Orihara and Ishibashi explaining the antiferroelectric phase transition in liquid crystals was developed considering the abovementioned peculiar behaviour exhibited by AFLC materials (*9*).

To the best of our knowledge, the material of our present interest, i.e. 1-ethylpropyl (*S*)-2-{6-[4-(4′-decyloxyphenyl)benzoyloxy]-2-naphthyl}propionate (EP10PBNP) appears to be the first AFLC with a chiral swallow-tailed molecular structure to exhibit V-shaped switching properties (*10, 11*). The V shape is found to be ferrielectric-like on cooling from the paraelectric chiral smectic A (SmA*) phase. However, the optical texture observation indicates an antiferroelectric chiral smectic C (SmC_A*) phase and thus the reported phase behaviour remains inconclusive. To remove the ambiguity, we have investigated the thermal hysteresis behaviour of the dielectric constant (ε'), electric field-induced dielectric loss spectra and polarisation measured with increasing and decreasing field in the SmA*–SmC_A* pre-transitional regime. Our results indicate the presence of a ferrielectric-like phase followed by an unstable antiferroelectric phase in the SmA*–SmC_A* pre-transitional regime.

2. Experimental

The sample used for our present investigation, i.e. 1-ethylpropyl (*S*)-2-{6-[4-(4′-decyloxyphenyl)benzoyloxy]-2-naphthyl}propionate (hereafter referred to as EP10PBNP), has the chemical structure and lowest energy conformation shown in Figure 1.

The phase sequence of EP10PBNP on cooling is: I 143.1°C BP_{II} 134.4°C N* 129.0°C TGBA* 128.2°C SmA* 102.5°C SmC_A* 54.2°C Cr (*10, 11*). Indium tin oxide (ITO)-coated transparent glass substrates were used as electrodes. Substrates were prepared by coating the glass plates with polyamide and baking at 140°C for 2 h. Homogeneously aligned samples were obtained by rubbing the substrate in one direction. Each cell was previously calibrated by using air and toluene as the standard references. The two cells of thicknesses 15 and 32 μm with active area 16 mm^2 of each cell were filled with EP10PBNP by means of capillary action using the isotropic liquid, as

*Corresponding author. Email: sspbkc@rediffmail.com

ISSN 0267-8292 print/ISSN 1366-5855 online

DOI: 10.1080/02678290802130231
http://www.informaworld.com

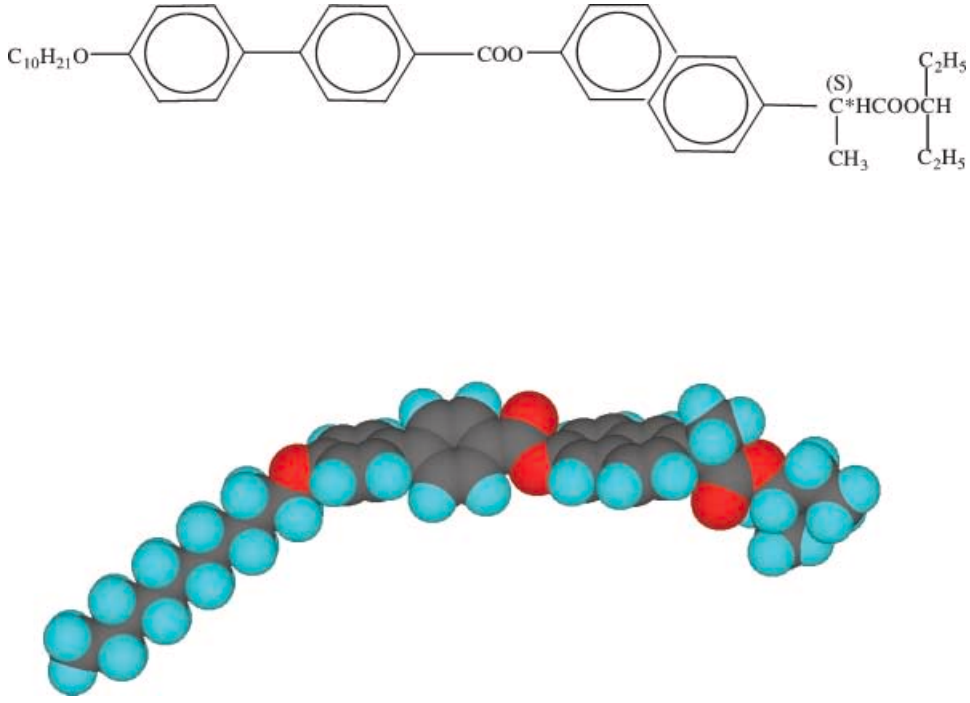

Figure 1. Structure and the lowest energy conformation for EP10PBNP obtained by semi-empirical calculations (AM1).

described in previous work (*12*). The sample under investigation was subjected to several cooling and heating cycles for better alignment. The measuring temperature was controlled by the Mettler FP82 hot stage along with Mettler FP90 temperature controller with an accuracy of $\pm 0.1^{\circ}$C. A computer-controlled HP 4192A impedance analyser was used for dielectric measurements. The spontaneous polarisation, P_S, was measured using a triangular wave method with a function generator (Model FG300, Yokogawa, Japan) and a homemade amplification arrangement (*13*). The values of P_S were evaluated by determining the area under the polarisation current peaks with respect to the baseline as follows

$$P_S = \frac{1}{2A}\int i(t)\mathrm{d}t, \qquad (1)$$

where A is the effective area of the sample in the cell.

3. Results and discussion

Figure 2 shows the temperature-dependent dielectric permittivity (ε') measured at 1 kHz. The sample under investigation was cooled from its isotropic phase at a rate of $0.1^{\circ}\mathrm{C\,min^{-1}}$ to the crystalline phase and simultaneously reheated to the isotropic phase at the same heating rate. The dielectric permittivity obtained in a pair of cooling/heating cycle (Figure 2) exhibits thermal hysteresis behaviour. The pronounced variation of ε' observed at 105°C confirms the SmA*–SmC_A* transition. The observed transition temperature is higher than that obtained by observation of optical texture by about 2.5°C due to the cell-imposed boundary conditions. Unlike the conventional paraelectric (SmA*) to antiferroelectric (SmC_A*) phase transition (*14*), the higher ε' value in the SmC_A* phase rather than that of the SmA* phase is considered to be "anomalous".

Interestingly, due to successive thermal cycles, the magnitude of ε' decreases significantly, confirming the process to be irreversible, and the process remains non-quasi static even at a cooling/heating rate of $0.1^{\circ}\mathrm{C\,min^{-1}}$. The unusual behaviour may be caused

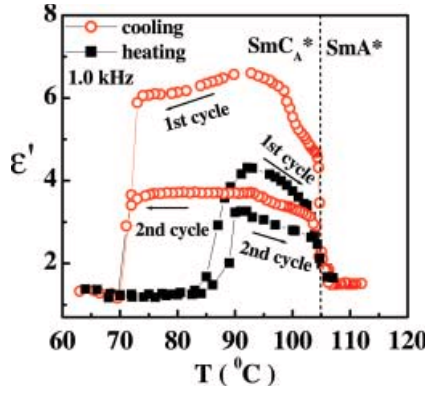

Figure 2. Temperature dependence of the dielectric constant (ε') for EP10PBNP at 1 kHz for heating and cooling runs at a rate of $0.1^{\circ}\mathrm{C\,min^{-1}}$.

either by a ferrielectric-like mesophase or by a sluggish molecular reorientation process in the pre-transition regime. In the following paragraph, we investigate the temperature- and electric field-dependent dielectric relaxation behaviour to reveal the fascinating molecular dynamics in the pre-transition regime.

The experimental dielectric data can be analysed using the Cole–Cole (*15*) modified Debye theory. According to this model, the angular frequency, ω ($=2\pi v$, where v is the linear frequency), dielectric strength, $\Delta\varepsilon=\varepsilon_S-\varepsilon_\infty$, ($\varepsilon_S$ is the static dielectric permittivity and ε_∞ is the high-frequency dielectric constant), and relaxation time, $\tau=1/2\pi v_c$ (where v_c is the relaxation peak frequency), obey the following relationship

$$\varepsilon^* - \varepsilon_\infty = \frac{\Delta\varepsilon}{1+(i\omega\tau)^{(1-\alpha)}}, \qquad (2)$$

where the complex dielectric permittivity (ε^*) can be expressed as

$$\varepsilon^* = \varepsilon'(\omega, T) - i\varepsilon''(\omega, T), \qquad (3)$$

T is the temperature and the parameter α measures the distribution of relaxation times ($0 \leqslant \alpha \leqslant 1$). $\alpha=0$ represents a single relaxation time, whereas its higher values measure the extent of distribution of relaxation times. It is well known that the contribution of ionic conduction is higher at lower frequencies. Its frequency dependence can be expressed (*16*) by

$$\varepsilon''(\omega) = \frac{\delta_0}{\varepsilon_0 \omega^{(1-S)}}, \qquad (4)$$

where δ_0 and S are fitting parameters. The power law exponent S is generally less than one, indicating a polaron hopping type of conduction mechanism. It appears that the conductivity contribution covers all the processes. However, by considering conduction a qualitative explanation of the relaxation mechanism is possible.

Figure 3 depicts the temperature-dependent behaviour of both v_c and $\Delta\varepsilon$ for the EP10PBNP sample.

With decreasing temperature in the SmA* phase, $\Delta\varepsilon$ increases and v_c decreases sharply as a signature of the soft mode (SM) (*17*). However, below the characteristic transition temperature (105°C), as obtained from the previous ε'–T plot (Figure 2), the thermal variation of $\Delta\varepsilon$ becomes slower. Two characteristic loss peaks (P_L and P_H) in the kHz and MHz ranges are, in general, observed in the dielectric spectrum of the SmC_A* phase (*18, 19*). However, we observe a single peak, having v_c varying

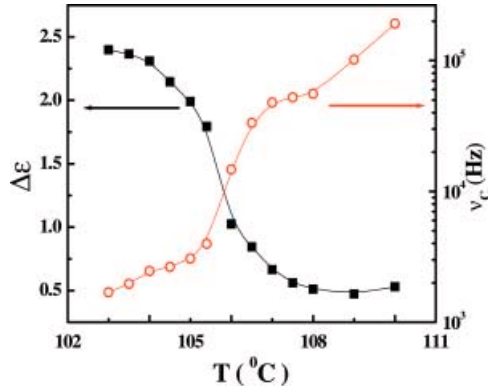

Figure 3. Temperature-dependent dielectric strength ($\Delta\varepsilon$) and relaxation frequency (v) for EP10PBNP.

between 1900 to 1.6 kHz, which is in contrast to the usual behaviour of AFLCs. The parameter α obtained in the fitting process lies in the range 0.15–0.28, indicating a non-Debye type of relaxation process.

As already mentioned, in the vicinity of the SmA*–SmC_A* transition, the loss peak is associated with a soft mode, appearing due to fluctuation of the molecular tilt. Figure 4 a represents the ε''–$\log_{10}(v)$ profile under various fixed dc bias fields at 105.4°C. The scattered points represent the experimental data and the continuous lines are theoretically fitted curves obtained using equations (3)–(4). The loss peak is found to shift towards the higher frequency side with increasing dc bias.

The variation of dielectric parameters $\Delta\varepsilon$ and v_c as a function of applied dc bias at 105.4°C and 106.0°C is shown in Figure 4 b. Whereas $\Delta\varepsilon$ decreases, v_c increases in a nonlinear manner with increasing field. The nonlinearity of $\Delta\varepsilon$ and v_c increases approaching the SmA*–SmC_A* transition temperature. The coupling between molecular tilts to the applied field causes this fluctuation. The previously mentioned nonlinear behaviour is caused by an electroclinic effect (*20*). Approaching the SmA*–SmC_A* transition temperature, the SmA* phase is softened, causing enhancement of the tilt fluctuation and thus nonlinearity is obtained both in $\Delta\varepsilon$ and v_c.

As the sample temperature is reduced below 105°C, one single mode is observed in the $\varepsilon''-\log_{10}(v)$ profile at 104°C, as shown in Figure 5. The mode strength increases under low bias field (~0.8 V) and then it is gradually suppressed with further increase of bias field (>0.8 V). Application of very low bias does not distort the macroscopic molecular structure, but provides stability to the unstable arrangement just after the SmA*–SmC_A* phase transition. But as the applied bias field is increased, the metastable helical structure continues to unwind, causing the

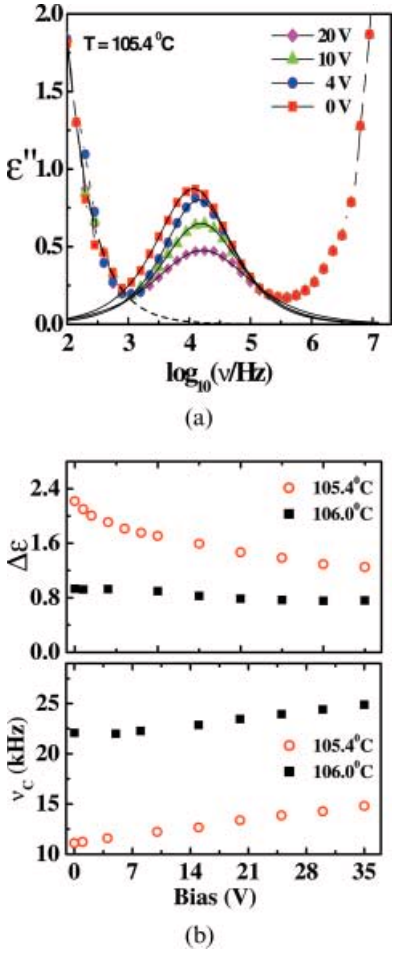

Figure 4 (a) Frequency (ν) dependence of the dielectric loss (ε'') in the SmA* phase at different fixed bias fields at 105.4°C for a 15 µm thick cell for the EP10PBNP sample. The dotted line shows the conductivity contribution [using equation (3)] with parameters $\delta_0 = 9.04 \times 10^{-11}$ and $S = 0.021$. The solid line shows the Cole–Cole fitting [equation (2)]. (b) Bias field dependence of dielectric strength ($\Delta\varepsilon$) and relaxation frequency (ν) of soft mode in the SmA* phase measured at 105.4°C for EP10PBNP.

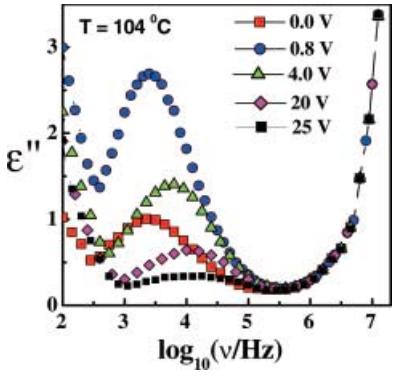

Figure 5. Frequency (ν) dependence of the dielectric loss (ε'') in the SmA*–SmC$_A$* pre-transition regime (104°C) at different fixed bias field for a 15 µm thick cell.

dielectric loss spectra to suppress and finally disappear as in the ferroelectric phase (*21*).

The dielectric loss spectra exhibit electric field-dependent behaviour similar to that of a ferrielectric phase (*22*). Thus, by analogy, dielectric investigation reveals a ferrielectric-like intermediate phase in the SmA*–SmC$_A$* pre-transition regime of the newly synthesised chiral swallow-tailed AFLC sample of our present investigation. However, the dielectric relaxation is observed within a very short range of temperature (~7°C) and to confirm this ferrielectric-like behaviour one needs further investigation, as revealed from our subsequent discussion.

To confirm the anomalous dielectric behaviour exhibited by the present sample, we investigated polarisation with increasing and decreasing electric fields in the pre-transition regime. The normalised values of spontaneous polarisation (NP) are plotted versus the applied electric field in the pre-transition regime at 104, 103, 100 and 98°C (Figure 6 a) and at temperatures of 96 and 92°C (Figure 6 b), which are away from the transition.

Interestingly, a sharp jump in the NP to one third of its maximum value (unwound SmC*) is observed (Figure 6 a) at an applied field of 0.8 V µm^{-1}, which corresponds to a stable field induced ferrielectric phase at $T = 104$°C. The competition between the field-induced and the temperature-induced molecular structure is responsible for this ferrielectric-like behaviour. At 103°C, the stable ferrielectric ordering is weakened as the region of stable field-induced NP$_{max}$/3 regime becomes narrow. However, at 100 and 98°C, hysteresis is obtained in the NP as the applied electric field is successively increased and then decreased. This observation shows the existence of domains and/or irreversible field-induced changes in the structure. Thus, temperature- and/or field-induced domains (likely to be ferroelectric) in the antiferroelectric macrostructure might be responsible for the observed irreversibility in the field-induced polarisation. As we cool the sample, the structural instability decreases and hence bifurcation between the measured polarisations (in the increasing and decreasing field conditions) decrease. At 96°C, for a bias field $E < 1$ V µm^{-1}, the polarisation is zero, indicating that the antiferroelectric phase is stable. When the field is increased, a linear increase in NP is obtained, as shown in Figure 6 b. The small plateau in the field-induced NP profile at ~2.6 V µm^{-1} (at 96°C) indicates a field-induced metastable state and NP finally saturates at ~3.4 V µm^{-1}. At 92°C, the field threshold enhances up to 1.2 V µm^{-1}, metastability vanishes and a stable structure is obtained. The hysteresis between the NP values measured with increasing and decreasing fields disappear due to

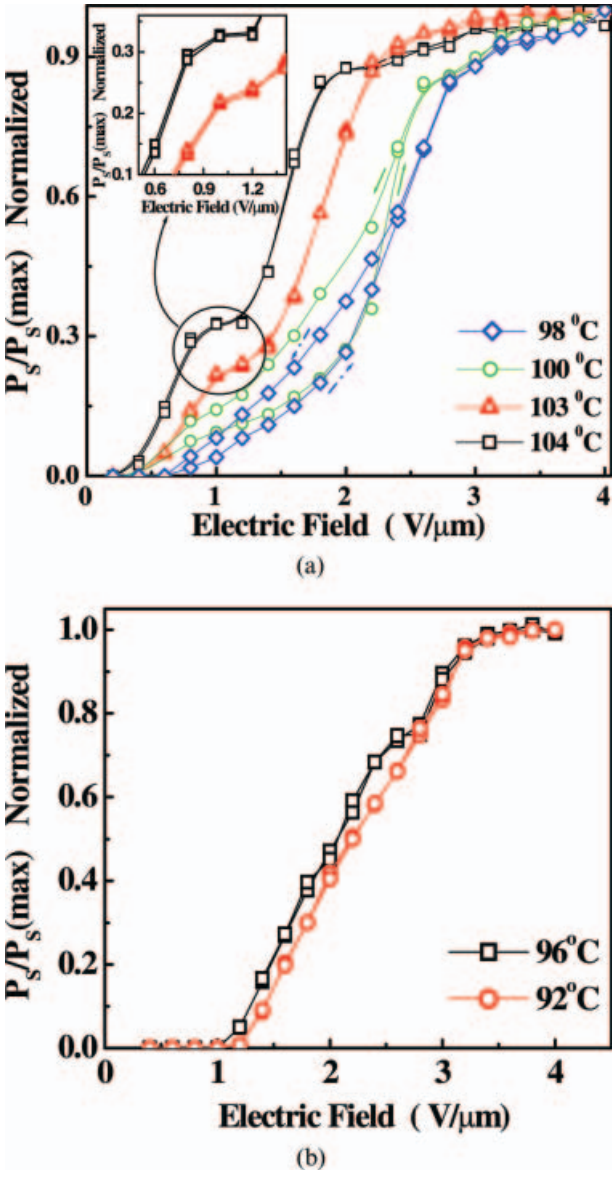

Figure 6. (a) Normalised spontaneous polarisation at various temperatures, as a function of applied field in the pre-transition regime of the SmA*–SmC_A* phases for EP10PBNP in a 15 μm thick cell. (b) Normalised spontaneous polarisation at 96°C and 92°C as a function of applied field away from the transition in EP10PBNP in a 15 μm thick cell.

increased stability of the antiferroelectric ordering at this temperature.

Thus, from the present dielectric and polarisation results, we confirm that in between the stable SmA* (paraelectric) and SmC_A* (antiferroelectric) states, the sample successively exhibits ferrielectric-like (<105°C to 103°C) and unstable antiferroelectric-like phases (<103°C to >96°C). The observed anomaly in the ε'–T plot in the pre-transitional regime (shown in Figure 2) is, therefore, caused by the above mentioned molecular ordering.

4. Summary and conclusion

The temperature- and bias field-dependent dielectric relaxation and spontaneous polarisation of a chiral swallow-tailed antiferroelectric liquid crystal, i.e. EP10PBNP, have been investigated. The Cole–Cole model fitting of the field-dependent dielectric loss, in the critical regime, reveals an electroclinic effect in the paraelectric (SmA*) phase. The observed thermal hysteresis behaviour of ε' in the consecutive cooling–heating cycles, the field-induced anomaly in dielectric loss spectra [ε''–$\log_{10}(\nu)$ plot] at 104°C and polarisation measurements revealed the existence of a ferrielectric-like intermediate phase followed by an unstable antiferroelectric ordering in between the stable SmC_A*–SmA* phases of the sample. However, further experimental confirmation would be important for a better understanding of the precise phase behaviour of this interesting sample.

Acknowledgments

The authors are grateful to Council of Scientific and Industrial Research for their financial support. The authors also acknowledge the AvH foundation for providing dielectric measuring instrument (HP4192A).

References

(1) Inui S.; Iimura N.; Suzuki T.; Iwane H.; Miyachi K.; Takanishi Y.; Fukuda A. *J. Mater. Chem.* **1996**, *6*, 671–673.
(2) Goodby J.W.; Slaney A.J.; Booth C.J.; Nishiyama I.; Vuijk J.D.; Styring P.; Toyne K.J. *Mol. Cryst. Liq. Cryst.* **1994**, *243*, 231–298.
(3) Nishiyama I.; Goodby J.W. *J. Mater. Chem.* **1992**, *2*, 1015–1023.
(4) Booth C.J.; Dunmur D.A.; Goodby J.W.; Haley J.; Toyne K.J. *Liq. Cryst.* **1996**, *20*, 387–392.
(5) Chandani A.D.L.; Ouchi Y.; Takezoe H.; Fukuda A.; Terashima K.; Furukawa K.; Kishi A. *Jap. J. Appl. Phys.* **1989**, *28*, L1261–L1264.
(6) Chandani A.D.L.; Gorecka E.; Ouchi Y.; Takezoe H.; Fukuda A. *Jap. J. Appl. Phys.* **1989**, *28*, L1265–L1268.
(7) Fukui M.; Orihara H.; Yamada Y.; Yamamoto N.; Ishibashi Y. *Jap. J. Appl. Phys.* **1989**, *28*, L849–L850.
(8) Fujikawa T.; Orihara H.; Ishibashi Y.; Yamada Y.; Yamamoto N.; Mori K.; Nakamura K.; Suzuki Y.; Hagiwara T.; Kawamura I. *Jap. J. Appl. Phys.* **1991**, *30*, 2826–2831.
(9) Orihara H.; Ishibashi Y. *Jap. J. Appl. Phys.* **1990**, *29*, L115–L118.
(10) Wu S.L.; Hsieh W.J. *Chem. Mater.* **1999**, *11*, 852–854.
(11) Wu S.L.; Chang P.L. *Liq. Cryst.* **2002**, *29*, 1355–1359.
(12) Kundu S.K.; Chaudhuri B.K.; Seed A.; Jakli A. *Phys. Rev. E* **2003**, *67*, 0417041–5.

(13) Miyasato K.; Abe S.; Takezoe H.; Fukuda A.; Kuze E. *Jap. J. Appl. Phys.* **1983**, *22*, L661–L663.
(14) Orihara H.; Fujikawa T.; Ishibashi Y.; Yamada Y.; Yamamoto N.; Mori K.; Nakamura K.; Suzuki Y.; Hagiwara T.; Kawamura I. *Jap. J. Appl. Phys.* **1990**, *29*, L333–L335.
(15) Cole K.S.; Cole R.H. *J. Chem. Phys.* **1941**, *9*, 341–351.
(16) Mott N.F.; Davis E.A. *Electronic Processes in Non-crystalline Materials*; Clarendon Press: Oxford, 1979.
(17) Hiller S.; Biradar A.M.; Wrobel S.; Haase W. *Phys. Rev. E* **1996**, *53*, 641–649.
(18) Buivydas M.; Gouda F.; Andersson G.; Lagerwall S.T.; Stebler B.; Bomelburg J.; Heppke G.; Gestblom B. *Liq. Cryst.* **1997**, *23*, 723–739.
(19) Panarin Y.P.; Kalinovskaya O.; Vij J.K. *Liq. Cryst.* **1998**, *25*, 241–252.
(20) Kalmykov Y.P.; Vij J.K.; Xu H.; Rappaport A.; Wand M.D. *Phys. Rev. E* **1994**, *50*, 2109–2114.
(21) Kundu S.K.; Suzuki K.; Chaudhuri B.K. *Ferroelectrics* **2003**, *287*, 47–61.
(22) Hou J.; Schacht J.; Giebelmann F.; Zugenmaier P. *Liq. Cryst.* **1997**, *22*, 409–417.